Structural Engineering and Mechanics, *Vol. 53, No. 6 (2015) 1083-1104*
DOI: http://dx.doi.org/10.12989/sem.2015.53.6.1083

Flexural strengthening of continuous unbonded post-tensioned concrete beams with end-anchored CFRP laminates

Saeed Ghasemi[1a], Ali A. Maghsoudi[1b], Habib A. Bengar[*2] and Hamid R. Ronagh[3c]

[1]*Civil Engineering Department, Shahid Bahonar University, Kerman, Iran*
[2]*Civil Engineering Department, University of Mazandaran, Mazandaran, Iran*
[3]*Civil Engineering Department, University of Queensland, Australia*

(Received November 11, 2013, Revised August 5, 2014, Accepted October 2, 2014)

Abstract. This paper provides the results of an experimental investigation into the flexural behavior of continuous two-span unbonded post-tensioned high strength concrete (HSC) beams, strengthened by end-anchored CFRP laminates of different configurations in the hogging region. Implementing two different configurations of end-anchorage systems consisting of steel plates and bolts and carefully monitoring the development of strains throughout the load history using sufficiently large number of strain gauges, the response of beams including the observed crack propagations, beam deflection, modes of failure, capacity enhancement at service and ultimate and the amount of moment redistribution are measured, presented and discussed. The study is appropriate in the sense that it covers the more commonly occurring two span beams instead of the simply supported beams investigated by others. The experiments reconfirmed the finding of others that proper installation of composite strengthening system is most important in the quality of the bond which is essential for the internal transfer of forces. It was also found that for the tested two span continuous beams, the capacity enhancement is more pronounced at the serviceability level than the ultimate. This is an important finding as the design of these beams is mostly governed by the serviceability limit state signifying the appropriateness of the suggested strengthening method. The paper provides quantitative data on the amount of this capacity enhancement.

Keywords: strengthening; CFRP laminate; HSC; unbonded post-tensioned; continuous beams; EBR

1. Introduction

During the last two decades, a great amount of experimental, numerical and analytical studies has been conducted on the behavior of simply-supported and continuous reinforced concrete (RC) beams, frames slabs and columns that were strengthened with fiber reinforced polymer (FRP) composites (Meier *et al*. 1993, Teng *et al*. 2002, Foret and Limam 2008, Lignola *et al*. 2007, El-Refaie *et al*. 2003, Farahbod and Mostofinejad 2010). These studies have proven that

∗Corresponding author, Assistant Professor, E-mail: h.akbarzadeh@umz.ac.ir
[a]Graduate Student, E-mail: S_ghasemi@eng.uk.ac.ir
[b]Associate Professor, E-mail: Maghsoudi.a.a@mail.uk.ac.ir
[c]Senior Lecturer, E-mail: h.ronagh@uq.edu.au

http://www.techno-press.org/?journal=sem&subpage=8 ISSN: 1225-4568 (Print), 1598-6217 (Online)

strengthening of reinforced concrete with FRP composites is a viable technique superior to more traditional methods in terms of installation time and overall life cycle cost of repair. The more common type of FRP used for strengthening purposes is the carbon fiber reinforced polymer (CFRP) which is available as pre-cured bars, strips, and tendons, as well as wet lay-up sheets. Some of the major benefits of CFRP include high strength to weight ratio, high fatigue endurance and ease of installation (ACI-440.2R-08, Rosenboom *et al*. 2007). To improve the load carrying capacity and the serviceability of beams, quality of the bond between concrete and laminate is important and it highly depends on proper installation of the composite (Rosenboom *et al*. 2009, Mirmiran *et al*. 2004). The system must be designed to avoid premature failure due to delamination or debonding of the CFRP material from the concrete surface. Premature bond failures such as plate-end (PE) debonding and intermediate crack (IC) debonding can significantly limit the capacity enhancement and prevent the full ultimate flexural capacity of the retrofitted beams to be attained. Several studies were conducted to identify ways of preventing premature failures with a view to improve the load capacity and ductility of strengthened concrete beams and preclude failure by debonding of the composites. A number of researchers have recommended the use of steel anchor bolts, steel clamps at the strip ends and mechanical fasteners in order to prevent premature failure of RC beams strengthened with FRP plates (Chahrour and Soudki 2005, Garden and Hollaway 1998, Lamanna *et al*. 2001, Bank and Arora 2006, Breña *et al*. 2003).

With the increasing use of high-strength/high-performance concrete (HSC/HPC) technology, researchers have started looking at the issues related to external FRP strengthening of reinforced concrete (RC) and prestressed concrete (PC) members constructed by HSC (Akbarzadeh and Maghsoudi 2010, Pellegrino and Modena 2009). The current study is also an attempt in that direction but focuses on strengthening of PC members.

Over the last few years, several studies on the strengthening of simply supported (determinate) prestressed concrete with CFRP laminates/sheets have been conducted (Rosenboom *et al*. 2009, Takács and Kanstad 2002, Rosenboom *et al*. 2007). Also there have been some field applications using CFRP to repair prestressed concrete that verified CFRP is an effective method for repairing/strengthening damaged PC girder bridges (Schiebel *et al*. 2001) and strengthening has reduced beam deflections in some cases by as much as 20% (Klaiber *et al*. 2003).

Rosenboom *et al*. (2007, 2009) conducted an extensive experimental program in several phases to study the behaviour of twenty two bonded PC bridge girders, which were tested under static and fatigue loading conditions by application of carbon fibre reinforced polymer (CFRP) and steel reinforced polymer (SRP) materials. They also suggested guidelines on the installation and inspection of composite strengthening systems of determinate PC members as well as structural design guidelines. Their findings indicated that SRP materials are more structurally efficient than (CFRP) materials. Their results also showed that the ultimate capacity of PC bridge girders can be increased by as much as 73% using CFRP without sacrificing the ductility of the original member. They presented an overview of installation procedures.

Chakrabari (2005) studied the repairing and retrofitting methods of determinate un-bonded post-tensioned beams using composite materials (GFRP and CFRP). Eleven 150 mm wide×250 mm deep×3600 mm long beams, were loaded to nearly their ultimate capacities. As the beams became i) noticeably cracked, or ii) when the deflections reached to twice the allowable deflection, or iii) the post-tensioning forces reached critical values; the beams were unloaded. The cracked beams were then repaired with varying amount of composite materials (carbon and e-glass) adhesives, and re-tested. Results of experiments revealed that the CFRP repair system provided more strength than the e-glass repair system.

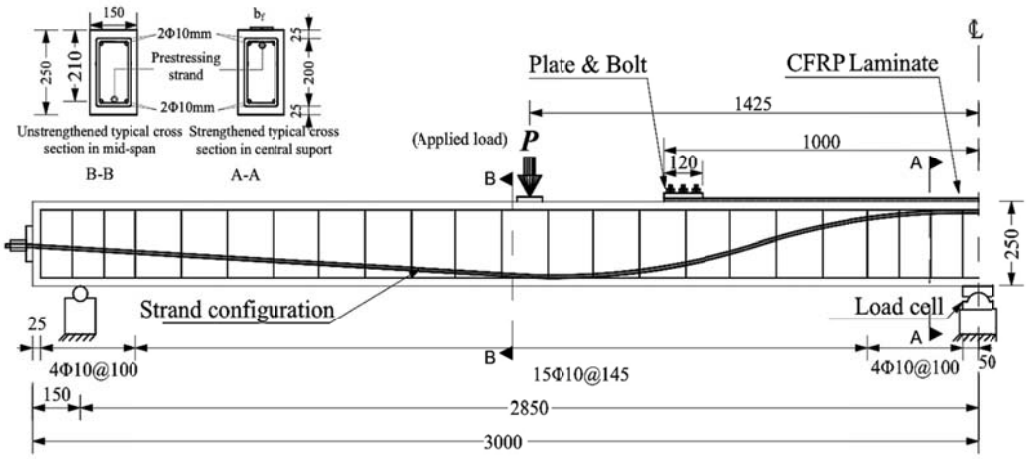

Fig. 1 Geometrical dimensions, Test set-up, Longitudinal profile, Typical cross section of beam in sagging and hogging region, End anchorageand reinforcement of test specimens (all dimensions in mm)

El Meski and Harajli (2012) conducted a study to evaluate the use of external FRP laminates for strengthening determinate unbonded post-tensioned concrete members. Twenty four full-scale simply supported beam and slab specimens reinforced with internal unbonded tendon system and strengthened using external FRP composites were tested. Additional twelve companion bonded PC and RC specimens were also tested for comparison. It was found that the use of FRP laminates increases the load capacity and post-cracking stiffness of unbonded members. The increase in load capacity was accompanied with reduction in deformation capacity. They indicated that provided a method is available for calculating the strains or stresses in the unbonded tendons at ultimate, the same guidelines reported by ACI-440.2R-08 for designing the FRP system for flexural strengthening of RC and bonded PC members can be applied for the unbonded members.

Although there are limited studies on strengthening of determinate unbonded post-tensioned concrete, and in spite of the fact that many in situ unbonded post-tensioned concrete beams are of continuous construction, based on the author's literature view, strengthening of unbonded continuous post-tensioned HSC beams with end-anchored pre-cured CFRP laminates, is yet to be studied theoretically or experimentally. Hence the focus of this research is on using FRP for flexural strengthening of continuous unbonded post-tensioned concrete structural systems.

An extensive experimental program was undertaken at Shahid Bahonar University of Kerman on 24 full-scale continuous unbonded post-tensioned concrete beams. Several parameters and their effects on the response were explored, including the area of external FRP reinforcement, span-to-depth ratio of the unbonded member, dimension of end anchorage device, cross section dimensions, type of concrete (normal and self-compacting concrete), configuration and method of strengthening. This paper presents the results of the first phase of this program on five girders; four which were strengthened with various CFRP areas and two types of end-anchorage plates, and one that was the control beam.

Aspects of the behavior investigated covered serviceability mode of flexural failure, ultimate load and deformation capacities, load-deflection response and load-strain responses of ordinary steel, internal strand, external FRP reinforcement and concrete of compressive zone. The experimental procedure, results and discussions are presented in the following.

2. Experimental procedure

2.1 Test specimens

Experiments were performed on five specimens of two-span un-bonded post-tensioned beams. The length of the beams were 6000 mm, and the sectional dimensions were 150×250 mm, as shown in Fig. 1.The beams contained two longitudinal steel bars of 10 mm at top and bottom. Area of prestressing strand based on cross section and length of concrete beam was selected 98.71 mm^2 (seven-wire stress-relieved strands- Grade 270). One beam was chosen as the control beam (CB); other beams were strengthened with CFRP laminates of 1.2 mm thickness. The widths of CFRP laminates were 30 mm for beams E30NA and E30NB and 50 mm for beams E50NA and E50NB, with a cross sectional area of 36 mm^2 and 60 mm^2 respectively. In this classification, E stands for the externally bonded reinforcement, N for strengthening of the negative moment region and finally A or B is used for two types of anchorage systems used (Figs. 2 and 3).The configuration of the laminate, reinforcements and longitudinal profile of tendon as well as the loading and support arrangements are shown in Fig. 1.

The beams details are presented in Tables1 and 2. In order to avoid shear failure in the beams, the closed stirrups were designed based on ACI-318-11 (2011) and more stirrups were provided at the end blocks as well as the central beam region (Fig. 1). In order to prevent the end-debonding failure, two types of end-anchorage systems (A and B) consisting steel plates and bolts were used.

The A type of anchorage system was consisted of seven bolts tightening two smooth surface base and bearing steel plates of 120×120×6 mm (Fig. 2). In this arrangement, the CFRP laminate was attached on the concrete surface, only by hand pressure with roller. However for the B type system, ten bolts with two rough surface base and bearing steel plates of 210×120×10 mm were used (Fig. 3). For this group a constant pressure of 7.6×10^{-3} MPa was applied during curing time of adhesive.

Table 1 Details of test beams

Beam no.	f'_{ci} (MPa)	f'_c (MPa)	Steel reinforcement		Prestressing steel area A_{p_s} (mm^2)	$\frac{f_{p_e}}{f_{p_u}}$
			Top	Bottom		
CB	51.1	68.1	2 bars of 10 mm diameter	2 bars of 10 mm diameter	98.71	0.47
E30NA	48.9	67.6				0.50
E50NA	49.2	67.9				0.52
E30NB	50.4	68.1				0.49
E50NB	48.3	67.7				0.53

Table 2 Details of control and strengthened beams

Beam no.	Over central support laminate				
	Width (mm)	Thickness (mm)	Area (mm^2)	Length (m)	End anchorage type
CB	None	None	None	None	None
E30NA	30	1.2	36	2	A
E50NA	50		60		A
E30NB	30		36		B
E50NB	50		60		B

(a) base plate and bolts

(b) bearing plate and end-anchored laminate

Fig. 2 End-anchorage system (A)

(a) base plate and bolts

(b) bearing plate and end-anchored laminate

Fig. 3 End-anchorage system (B)

The control beam (CB) had no external reinforcement. Table 2 presents the details of the CFRP laminates used in different beams. The laminates applied to the top surface of the beam were placed symmetrically about the central support so that only the negative moment region was strengthened. The process of application of CFRP laminate to concrete is summarized below:

a. The concrete surface was prepared with abrasive disk;

b. First grooves the size of the base plate on tension side of beam were graved. Then, base plate and six/ten bolts of 16 mm diameter and 60 mm length were embedded in groove on tension side of beams by adhesive (Figs. 2(a) and 3(a));

c. The two-component epoxy resin (thickness of 2 mm) was prepared in accordance with the manufacturer's recommendations;

d. The laminate was applied to the concrete tensile surface, pressing it down by hand pressure and rolled into the adhesive with a rubber roller for group A. A constant weight was added for group B during curing;

e. Bearing plate was used at the top of CFRP laminate to anchor the ends of laminates (Figs. 2(b) and 3(b));

f. The seventh bolt was added to anchor the CFRP laminates to the end of steel plates for group A.

g. The complete application was subsequently left to cure for a minimum of 10 days at room temperature before load testing of the beams.

2.2 Material properties

The beams were casted with high strength concrete, HSC. The concrete mix proportion is given in Table 3. For each beam, nine100×100×100 mm concrete cubes were made from each batch of concrete used to make the test beams. Those were kept at the same location as the beams during curing in order to eliminate the climate factor. The cubes were tested on the day of beam's post-tensioning operation ($f_{ci}^{'}$) and on the same day as the test beams in order to provide values of the cube strength (f_{cu}) (BS EN 12390-3 2009). The mean cylindrical concrete compressive strength ($f_{ci}^{'}$,$f_{c}^{'}$) for each beam is shown in Table 1. The relationship between cylinder strength ($f_{c}^{'}$) and cube strength was considered as $f_{c}^{'}$=0.85 f_{cu} (Iranian concrete code 2009).

The mechanical properties of the unidirectional CFRP laminates and epoxy adhesive obtained from the manufacturer's data sheets are summarized in Tables 4 and 5. The mechanical characterizations of prestressing and deformed steel used in the test specimens are described in Table 6. Prestressing steel was Grade 270 (1861.9 MPa) seven-wire stress-relieved strands.

Table 3 Concrete mixture proportions

Cement (kg/m^3)	Silica fume (kg/m^3)	Coarse aggregate (kg/m^3)	Fine aggregate (kg/m^3)	Super plasticizer (kg/m^3)
630	70	850	750	10.75

Table 4 Mechanical properties of the CFRP laminate

Material	Density (kg/cm^3)	Thickness (mm)	Ultimate Tensile stress f_{f_u}(MPa)	Young's Modulus E_f (GPa)	Ultimate strain ε_{f_u}(%)
CFRP	1.81	1.2	3000	165	1.7

Table 5 Mechanical properties of the epoxy adhesive

Compressive strength (N/mm^2)	Tensile strength (N/mm^2)	Flexural strength (N/mm^2)	Shear strength (N/mm^2)
95	31	71.1	19

Table 6 Mechanical properties of prestressing and deformed steel

Type of steel	Nominal diameter (mm)	Nominal Area (mm^2)	Yield strength f_y (N/mm^2)	Ultimate strength f_u (N/mm^2)	Modulus of elasticity E_s (kN/mm^2)	Nominal weight (kg/km)	Max. % Relaxation after 1000Hrs
Prestressing grade 270	11.21	98.71	1714	1925	195	740	2.5
Deformed steel	10 (mm) Top & Bottom steel bar	78.54	336	525	192.5	---	---

Table 7 Properties of different electrical resistance strain (ERS) gauges

Type of material	Type of ERS	Electrical resistance(Ω)	Length (mm)	Coefficient
Prestressed strands	FLK-2-11-5	120 ± 0.3Ω	2	2.10
Steel bars	FLA-10-11	120 ± 0.3Ω	10	2.09
CFRP laminate	BFLA-5-5	120 ± 0.3Ω	5	2.11
Concrete	PFL-30-11	120 ± 0.3Ω	30	2.13

2.3 Test setup and instrumentation used

Test beam comprising two equal spans of 2850 mm were loaded with a concentrated load at the middle of each two span as shown in Fig. 1. A hydraulic actuator was used to load the beam. The reaction of the beam at the central support was measured using a load cell. Disposable electrical resistance strain (ERS) gauges used were from TML and are given in Table 7. The ERS gauges were attached to the top and bottom of concrete surface of the beams at the mid-span and the central support respectively, to measure the extreme layer of concrete compressive strain (ε_c). The ERS gauges were also pasted on the tensile and compressive bars at the mid-span and the central support. The ERS gauges were used on six wires of strand (except the central wire) at the beginning, the end, the central support and the mid-span of the beams and at seven locations on the CFRP laminates from central support to end anchorage to monitor experimentally the development of material strains throughout the loading history.

Mid-span deflections were measured using linear variable differential transformers (LVDTs). For the tested beams, the load was applied step-by-step to failure in a load control manner. In other words, the load was applied in 5 to 10 kN increment up to failure. The experimental values were monitored using a data acquisition system and the data was recorded and stored in the computer. The crack widths were also measured by a crack detection microscope with an accuracy of 0.02 mm. At the end of each load increment, observations, measurements, crack development and its propagation on the beam surfaces were recorded.

To obtain the stress-strain diagram, the strands and rebars were tested in tension based on ASTM-A370-2012 (Ghasemi 2012). Approximately 1000 hours before the loading test, each prestressing strand was anchored at the far end and then tensioned from the prestressing end using a center hole hydraulic ram. The effective prestressed values after 1000 hours, f_{pe} (i.e., at the time of beams test) for all the beams which were monitored using the readings of the strain electrical gauges attached on the strands varied between about 47% and 53% of the ultimate strength of the strands (the more exact values are given in Table 1). This range of tension stress is representative of the effective stress f_{pe} available in the prestressing steel during the service life of the PC members after accounting for the long-term prestress losses.

3. Test results

The obtained experimental results are presented and subsequently discussed in terms of the observed crack propagation, beam deflection (serviceability) and mode of failure, enhancement of load and moment capacity at service and ultimate limit states and moment redistribution.

3.1 Serviceability states

Unlike RC, the primary analysis of PC is based on service conditions, and on the assumption that stresses in the extreme concrete fibers are limited to values which will correspond to elastic behavior (ACI-318-11, BS-8110 1997). If the tensile stress in the concrete is limited to a certain permissible value, then all stresses can be calculated on the assumption that the section is uncracked and thus the gross concrete section properties govern. If this is not the case, then calculations may have to be based on a cracked section. Limited cracking is permissible depending on whether the beam is pre- or post-tensioned and the appropriate exposure conditions. However, in BS (1997) for the design of prestressed flexural members, the three following classes are allowed under service loads. The flexural tensile stress and crack limitation for each class is: class 1; the stress is zero and no crack is allowed, class 2; the stress is calculated by Eqs. (1) and (2) for bonded and unbonded tendons respectively with non-visible cracks. For class 3; although cracking is allowed, it is assumed that the concrete section is uncracked and that design hypothetical tensile stresses exist at limiting crack widths of 0.1 mm and 0.2 mm with either prestressed or grouted (bonded) post-tensioned tendons, depending on the surrounding area conditions. No suggestion is given for unbonded post-tensioned tendons. For all classes, the compressive stress should not exceed $0.4f_{cu}$ for continuous beams.

$$f_t = 0.36\sqrt{f_{cu}} \tag{1}$$

$$f_t = 0.45\sqrt{f_{cu}} \tag{2}$$

In the case of strengthened beams, the provision of CFRP laminate resulted in an improved crack control, reduced deflection and improved serviceability in comparison to the un-strengthened control beam.

3.1.1 Cracking propagation

Post-tensioned concrete beams with fully unbounded reinforcement tend to develop few cracks and concentrate deformation on a single crack (at critical regions) during the beam's failure (Warwaruk *et al*. 1962). It is therefore, for better distribution of cracks for the tested beams of this report (especially for control beam,(CB)), 2Φ10 bars which is slightly more than the minimum area of ordinary steel reinforcement, based on the ACI-318-11 suggestion, Eq. (3) is used

$$A_s = 0.004A \tag{3}$$

Where A is that part of the cross section between the flexural tension face and the center of gravity of the gross section.

Considering the CB specimen (Fig. 4(a)), the first visible flexural crack occurred at the maximum moment region (i.e., at central support) with a crack width of 0.03 mm at the cracking load (P_{cr}) of 64.1 kN (Table 8). By slightly increasing the load, the cracking became extensive with only a limited number of cracks, and crack widths increased in this region. However, on further load increases, the cracks accrued under the load points at the two mid spans. Fig. 4(b) illustrates that the number of cracks occurring at the mid span were more than the number of cracks at the central support. The observed crack propagation in CB, is not similar to past research findings on RC (Akbarzadeh Bengar and Maghsoudi 2010) or bonded PC (Pellegrino and Modena 2009) due to strands having been unbonded.

As for the strengthened beams, the first flexural crack appeared under the load points in the mid

(a) at the central support (b) at the mid-span

Fig. 4 Crack pattern of CB

Table 8 Results of tested beams including cracking, yielding, ultimate load, failure mode and enhancement ratio (α, β, γ)

Beam no.	Cracking load			Yielding load		Ultimate load		Failure modes
	P_{cr} (kN)	w_{cr} (mm)	α	P_y (kN)	β	P_u (kN)	γ	
CB	64.1	0.03	1	113.9	1	218.55	1	Flexural failure
E30NA	83.1	0.02	1.29	132.1	1.16	236.2	1.08	Concrete crushing and end anchorage slipping
E50NA	94.9	0.04	1.48	160.4	1.41	251.65	1.15	Concrete crushing and end anchorage slipping
E30NB	88.5	0.03	1.38	141.2	1.24	242.6	1.11	Concrete crushing, end anchorage pull-off and FRP rupture
E50NB	100.2	0.03	1.56	169.1	1.48	262.3	1.20	Concrete crushing and end anchorage pull-off

α is ratio of the first cracking load of strengthened beams to that of control beam.
β is ratio of the steel bar yielding load at tension of strengthened beams to that of control beam
γ is ratio of the ultimate load of strengthened beams to that of control beam.

span regions and cracking load at the central support was increased in comparison with CB due to external strengthening of the hogging region. The cracking and yielding loads, the relative ratios of loads and initial crack widths of the tested beams are provided in Table 8. It is clear that the cracking loads are significantly higher than that of the CB with the P_{cr} of beams E30NA, E50NA, E30NB and E50NB being 83.1, 94.9, 88.5 and 100.2 kN respectively. The highest increase in the cracking load belongs to E50NB with an α of 1.56.

However, a close observation during the tests indicated that, for strengthened PC beams with CFRP laminate, new cracks appeared in between existing cracks, the number of flexural cracks and length of cracked regions were also increased (Fig. 5). (In other words as the load increased to failure, the cracks tended to fork out and additional flexural cracks formed). Hence, it can be concluded that the strengthening has resulted in denser cracking and smaller crack widths and has enhanced the beam's flexural capacity in comparison to CB.

Table 9 contains these enhanced load capacities corresponding to crack width enhancement. The loads corresponding to two permissible flexural crack widths of 0.1 and 0.2 mm based on BS (1997) limitations of class 2 and 3, and also for 0.3 and 0.4 mm are presented in Table 9. The load

Fig. 5 Crack pattern of the strengthened beams at the central support

Table 9 Total load correspond to various crack width and enhancement ratio (κ, λ, η, ξ)

Beam no.	w_{cr}=0.1		w_{cr}=0.2		w_{cr}=0.3		w_{cr}=0.4	
	P (kN)	κ	P (kN)	λ	P (kN)	η	P (kN)	ξ
CB	69.1	1	76.3	1	83.5	1	90.8	1
E30NA	96.7	1.40	110.4	1.45	124.2	1.49	135.9	1.50
E50NA	109.5	1.58	125.6	1.64	141.9	1.70	159.2	1.75
E30NB	101.8	1.47	117.5	1.54	130.1	1.56	145.1	1.60
E50NB	116.2	1.68	133.1	1.74	150.1	1.80	166.7	1.84

κ is ratio of load correspond to crack width 0.1 of strengthened beams to that of control beams at the central support

λ is ratio of load correspond to crack width 0.2 of strengthened beams to that of control beams at the central support

η is ratio of load correspond to crack width 0.3 of strengthened beams to that of control beams at the central support

ξ is ratio of load correspond to crack width 0.4 of strengthened beams to that of control beams at the central support

equal to the crack width of 0.1, 0.2, 0.3, 0.4 mm for beam E50NB, which shows the best performance, is increased by 1.68, 1.74, 1.80 and 1.84 of CB respectively.

3.1.2 Deflection

The total applied load versus deflection diagrams at the mid-span section is shown in Fig. 6. The curves indicate that the strengthened and the control continuous post-tensioned HSC beams, exhibit typical flexural behavior; three stages of straight lines with nearly different response up to failure. In stage 1, the curve represents the concrete pre cracking; in stage 2, concrete post cracking and tension steel pre yield (i.e., this stage starts at occurrence of initial crack up to yielding of ordinary reinforcement) and in stage 3, tension steel post yield and the failure. The load values for these three stages are presented in Table 8. Unlike the load-deflection behavior of continuous reinforced HSC beams of similar condition reported by Akbarzadeh Bengar and Maghsoudi (2010) the curve slope at stage 3 of CB is not horizontal. In other words, at the start of stage 3, due to the

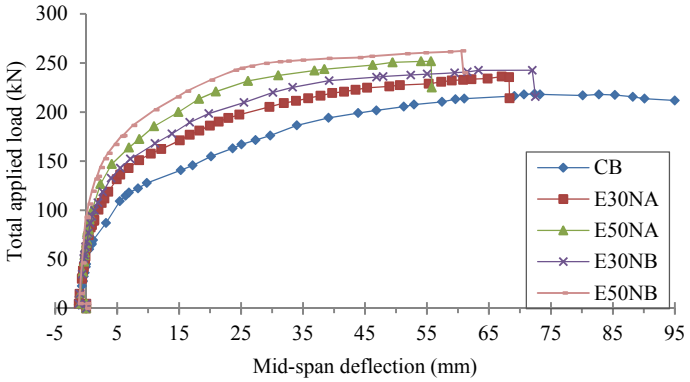

Fig. 6 Total applied load versus mid-span deflection for the tested beams

Table 10 Total load in accordance with allowable deflections and enhancement ratio (ψ, ϑ, χ, υ)

Beam no.	Δ=L/180=15.83 (mm)		Δ=L/240=11.88 (mm)		Δ=L/360=7.92 (mm)		Δ=L/480=5.94 (mm)	
	P (kN)	ψ	P (kN)	ϑ	P (kN)	χ	P (kN)	υ
CB	141.2	1	132.7	1	121.1	1	111.5	1
E30NA	173.6	1.23	161.6	1.22	147.9	1.22	138.8	1.24
E50NA	207.4	1.47	189.5	1.43	165.1	1.36	157.9	1.42
E30NB	185.6	1.31	170.2	1.28	156.2	1.29	145.2	1.30
E50NB	220.1	1.56	205.3	1.55	188.6	1.56	176.1	1.58

ψ is ratio of the load in accordance with deflection of L/180 of strengthened beams to that of control beam.
ϑ is ratio of the load in accordance with deflection of L/240 of strengthened beams to that of control beam.
χ is ratio of the load in accordance with deflection of L/360 of strengthened beams to that of control beam.
υ is ratio of the load in accordance with deflection of L/480 of strengthened beams to that of control beam.

presence of un-yielded unbonded tendon, there is a significant slope in the curve at this stage and a considerable deflection enhancement occurred by load increment up to failure (Fig. 6). In stage 2, a considerable difference exists between the CB and the strengthened beams. In CB, the initial crack occurred earlier with a rapid increase on the width of a limited number of cracks, whereas in the strengthened beams, a suitable distribution of cracks with smaller width and deflection occurred. A close observation during the tests revealed that upon beam cracking and yielding at the central support, IC debonding had also occurred. A small length of laminate debonded at the central support as the flexural intermediate cracks grew wider. The debonding length was increased as the loads were incremented higher resulting in larger rotation at the central support. The enhancement of the crack width, length of laminate debonding and rotation of the central support contributed to the mid span deflection. It can be concluded that external strengthening compensates for the unbonding of the strands and as such improves the serviceability of the beams. The beams deflections for system B were lower than those of system A (Fig. 6). In system B, there was a delay on debonding, and for the same load a shorter debonding length was formed.

In the open literature, one can find no trace of deflection prediction for continuous unbonded post-tensioned FRP-strengthened beams. Here, for the conventionally suggested limits of L/180, L/240, L/360 and L/480 (ACI 318-2011), the corresponding allowable load limitations are determined. For the beam with 2850 mm span, these workout to be 15.83, 11.88, 7.92, 5.94 mm

respectively. The values of experimental loads corresponding to theoretical allowable deflection limitations are presented in Table 10. Load factors, ψ, ϑ, χ and υ corresponding to each allowable deflection limitation are obtained and presented in Table 10. By increasing the area of CFRP laminates, beam's stiffness is increased; therefore, for the same value of an applied load, the mid-span deflection decreases as the area of CFRP laminates increases. It is clear that a considerable increase in the load factor can be achieved by strengthening the unbonded post-tensioned beams. The greatest load increment belongs to E50NB that increases by 58% relative to CB (the more exact values are given in Table 10).

3.2 Failure mode

The specimen's modes of failure are provided in Table 8. The failure modes of CB involved concrete crushing and yielding of steels and that of other beams were accompanied with other modes (Table 8). Failure of the strengthened unbonded PC specimens occurred either by FRP rupture, FRP debonding, anchorage failure or a combination of these. These modes of failure depended on the area of external FRP reinforcement relative to the area covered by the anchor plates and also the quality of the bond. Based on the strain measured in the tensile steel, concrete and CFRP laminates, the following observations can be made. Strain measurements of the tensile steel at the central support and the mid-span regions of CB revealed that, as predicted, a plastic hinge had been formed initially upon the yielding of the upper tensile steel at the central support. This yielding of the tensile steel was coincident with the growth of the flexural cracks and rotation of the beam in addition to a redistribution of moments from the central support towards the mid-span of the beam. The tensile steel at the bottom of the mid-span then reached its yielding point with cracks well extending into the compressive regions. At failure, the compressive concrete strain at the central support and the mid span reached high values of 5110 $\mu\varepsilon$ and 4800 $\mu\varepsilon$ respectively and the beam failed in a flexural mode. After crushing of concrete in the compressive region, the width of cracks at the central support and at the mid span, reached 13 and 15 mm respectively for a deflection of 100 mm (Fig. 6) before the load was stopped.

In the group A strengthened beams (for E30NA and E50NA specimens), the first crack occurred at the mid-span and on further increasing of the loads, the crack opened at the central

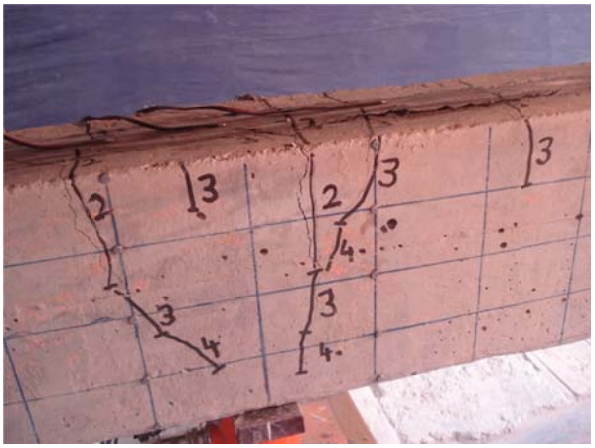

Fig. 7 Visible debonding of laminate in E30NA (IC debonding, no concrete cover separation)

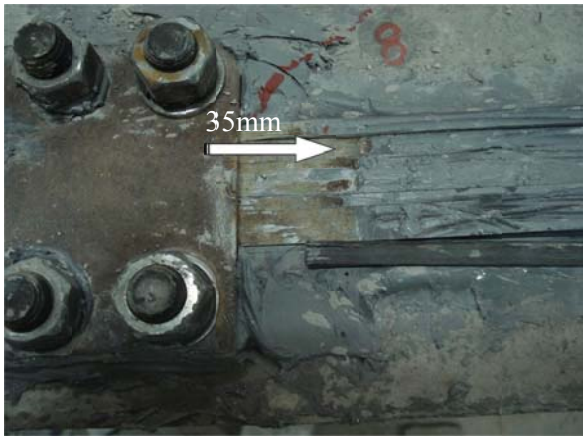

Fig. 8 End-anchorage failure of beam E50NA (laminate slipping)

Fig. 9 End-anchorage failure of beam E30NB (end-anchorage pull-off and FRP rupture)

support. Upon yielding of the tensile steel at the central support, as the flexural intermediate cracks grew wider in this region, the FRP started to debond at 130 and 158 kN for E30NA and E50NA specimens respectively. Upon debonding, the measured FRP strains were 6300 με and 6900 με for E30NA and E50NA respectively. With increasing the load, the visible debonding length also increased gradually (Fig. 7). The trend continued until at 195 and 211 kN (for E30NA and E50NA specimens respectively) the laminates totally debonded from the concrete surface as flexural intermediate cracks at the top of the central support region grew too wide with only the end-anchorage device standing intact. Finally, failure occurred when the end anchorage device failed to carry any more load. The mechanical anchorage devices lost their resistance and a small laminate slippage occurred between the end plates and the laminate (Fig. 8). Upon slipping (i.e., at failure), the measured FRP strains were 8450 με, 6833 με for E30NA and E50NA respectively.

In the group B strengthened beams (for E30NB and E50NB specimens), the first crack occurred at the mid-span and on further increasing the load, a new crack was opened at the central support. Table 8 shows the small load increment at the first crack for group B compared to the group A. Upon yielding of the tensile steel at the central support, as the flexural intermediate cracks grew wider in this region and went through the strengthened region, (unlike group A) there

Fig. 10 Failure of beam E50NB (debonding accompanied with the concrete cover separation)

was no visible debonding length along the loading history up to failure in group B. Finally, after concrete crushing at the mid-span under the load points, failure occurred suddenly with damage of the anchorage device resulting in the loss of load carrying capability. The mechanical anchors lost their resistance and the end plates were pulled off the concrete.In the specimen E30NB, this pull-off was followed by FRP debonding and partial rupture of the FRP (Fig. 9) in addition to concrete crushing at the central support; for E50NB the pull-off was followed by debonding accompanied the concrete cover separations (Fig. 10) and concrete crushing at the central support.

Upon pull-off (i.e., at failure), the measured FRP strains was 9600 με and 8255 με for E30NB and E50NB respectively. According to ACI-440.2R-08 in order to prevent such an intermediate crack-induced debonding failure mode, the effective strain in FRP reinforcement should be limited to the strain level given by Eq. (4).

$$\varepsilon_{fd} = 0.41\sqrt{\frac{f_c'}{nE_f t_f}} \leq 0.9\varepsilon_{fu} \tag{4}$$

The measured FRP strain for group A of the tested beams upon debonding was significantly lower than the recommended value (7500 με) using Eq. (4). It is worth mentioning that in ACI-440.2R-08 there is no specific formula for FRP strain in unbonded post-tensioned beams. Comparing the failure loads found from the experimental measurements of groups A and B and observing the failure modes of the two mechanical anchorage systems, it can be concluded that group B has a superior performance. The group B failure loads are generally higher than those of group A and no laminate slipping occurs in group B.

3.3 Load–strain response

The total applied load versus extreme concrete compressive strain, CFRP laminate strain, tensile steel bar and post-tensioned unbonded strand strain at the central support of continuous tested beams are plotted and shown in Figs. 11 to 14, where the negative sign is considered for the concrete compressive strain.

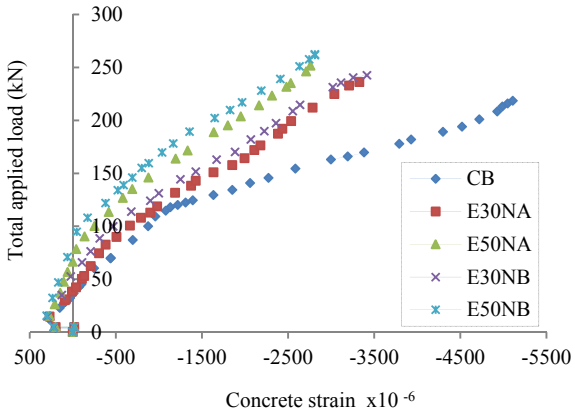

Fig. 11 Load versus extreme concrete compressive strain at the central support of test beams

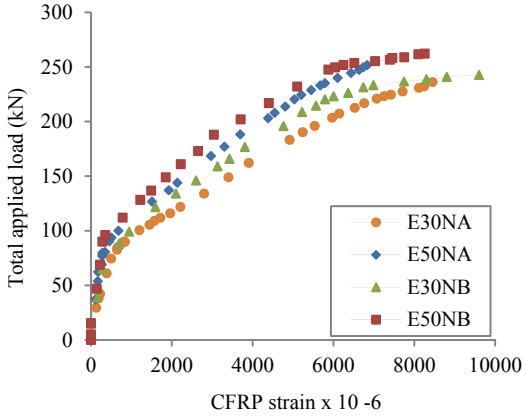

Fig. 12 Load versus tensile strain at the middle of CFRP laminates (i.e., central support of test beams)

3.3.1 Extreme concrete compressive strain

For the tested beams, the concrete compressive strains measured using at least four electrical strain gauges attached on the bottom and on the sides of the concrete beam, very close to the mid span and to the central support. Fig. 11 indicates the strain of concrete bottom surface at the central support. The highest strain value is for CB with a value of 5110 $\mu\varepsilon$, which is considerably higher than the suggested values of different design codes (ACI-318-11, BS-8110 1997). The results indicate that the provision of A_s'=2Φ10 and stirrups, Φ10@10cm centers at the central support region for a length of 700 mm, was capable of affecting the beam confinement. For the strengthened beams, the concrete compressive strain independent of the area of CFRP laminate remains more or less linear up to the beam's failure and is not significantly affected by concrete cracking or yielding of the tensile steel. These results demonstrate that the effect of strengthening is to reduce the strain in the compressive region of concrete. Thus, externally bonded FRP laminate may also be utilised to reduce concrete compressive stresses, in addition to acting as additional tensile reinforcement.

Comparison between the amount of concrete compressive strain for two anchorage system, A and B (Fig. 11) indicates that, for a particular load, the strain value is reduced for system B. This is

due to the occurrence of a smaller rotation in the critical region at the central support, a lower deflection and also the delay in laminate debonding of beams in group B. The measured concrete compressive strain values for E30NA, E50NA, E30NB and E50NB beams were respectively 3327 με, 2760 με, 3415 με and 2812 με.

3.3.2 CFRP laminate strain

The tensile strain in CFRP laminates was measured from end anchorage to central support by using seven electrical strain gauges. Fig. 12 indicates the CFRP tensile strain at the central support. Tensile strains in the FRP laminates were increased significantly after concrete cracking. In addition, the strain of FRP laminates rapidly increased after yielding of the internal tensile steel reinforcement. Not only increasing the area of laminate reduced the tensile strain of the laminate for a given value of the applied load, but it also decreased the maximum tensile strains in the laminates before the beam failure (Fig. 12). The measured laminate strain values for beams; E30NA, E50NA, E30NB and E50NB were 8450 με, 6833 με, 9600 με and 8255 με respectively. The FRP strain corresponding to the applied load (including the ultimate state) generally decreased with the increase in the area of FRP reinforcement (Fig. 12). For the type B anchorage, at a particular value of the applied load, laminates tensile strain reduced when compared to the type A anchorage. As for group B, there is no surface slippage of laminate and the maximum tensile strains of laminates are increased prior to the beam's failure (Fig. 12).

3.3.3 Internal tensile steel strain

Fig. 13 shows the total applied load against the tensile strain in the top steel bars at the central support of the beams. It indicates that the total applied load, at which the tensile steel bars of the strengthened beams yielded, was higher compared to that of the control beam. In the strengthened beams, the FRP laminates increased the beams rigidity so that after yielding of the tensile steel reinforcement, the beam continues to carry load and the slope of load-deformation curve does not drop to near zero as is the case for the control beam, CB (Fig 13). In addition, for a given load, the strain in the ordinary steel is reduced compared to CB (Fig 13). The measured steel tensile strain values for beams; CB, E30NA, E50NA, E30NB and E50NB were 17884 με, 8309 με, 6377 με, 8761 με and 6900 με respectively. Comparing the strain of steel for the two anchorage systems, A and B (Fig. 13) indicates that, at a particular load because of the delay in the FRP laminate debonding and the lack of slippage at the anchorage steel plates, the amount of beam rotation at the central support and the steel strain are smaller for group B.

3.3.4 Post-tensioned strand strain

The load versus post-tensioned strand strain of the tested beams is shown in Fig. 14. It indicates that before testing of the beams, only the beams self-weight was acting as the external load and the range of strand effective strains after total prestress loss, was between 4668 με and 5156 με. Comparing Figs. 6 and 14, it is seen that the curve for the applied load versus unbonded strand strain enhancement follows a trend similar to that of load-deflection response, which indicates there is a close relation between deflection and stress in the unbonded post-tensioned tendons. While only the control unbonded beam developed a level of strain passing yield at the onset of failure, the strengthened beams in groups A and B, experienced strain values close to yield at failure. At the peak load, the value of strain or stress in the unbonded strands generally decreased with an increase in the area of external FRP reinforcement for the beam with the same end anchorage system (Fig. 14). The measured strand strain values for beams; CB, E30NA, E50NA,

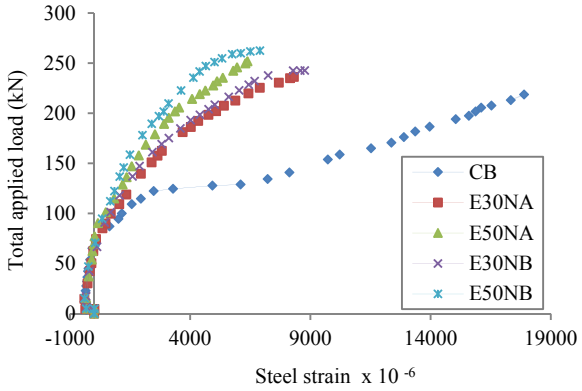

Fig. 13 Load versus top tensile steel strain at the central support of test beams

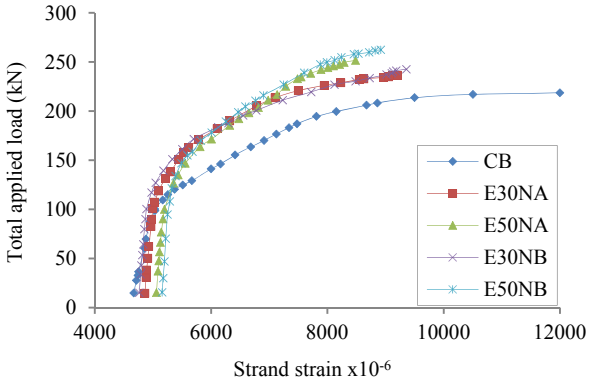

Fig. 14 Load versus post-tensioned unbonded strand strain at the central support of test beams

E30NB and E50NB at ultimate load were 12000 με, 9200 με, 8485 με, 9358 με and 8920 με respectively.

3.4 Enhancement of load and moment

The failure load results and the ultimate load enhancement ratio γ, which is defined as the ratio of the ultimate load of a strengthened beam to that of the CB, are summarized in Table 8. It indicates that using CFRP laminates in the negative region to strengthen of continuous unbonded post-tensioned beams, is not only an effective technique to improve the serviceability considerations, but also it improves the load resistance capacity as the ultimate load for E30NA, E50NA, E30NB and E50NB increased by a factor of 1.08, 1.15, 1.11 and 1.2 respectively in comparison with CB. Fig. 6 presents the curves for the total loads exerted on each beam in terms of the corresponding mid-span displacement. It should be noted that the strengthening increased the beams rigidity so that the mid-span displacement in the strengthened beams reduced in comparison to the control beam. Smaller deflection, in turn, resulted in smaller values of the strand strain. It is therefore concluded that the strand strain in the strengthened beams does not increase as much as that of the CB which is more dependent on the ultimate load condition. Another observation here is that the highest load carrying capacity belonged to the group B (E50NB).

Comparing the two mechanical anchorage systems A and B, for the same area of CFRP laminate (the beams, E50NB and E50NA); the load carrying capacity of system B was higher by 5%. Table 11 lists the ultimate moment and its enhancement ratio μ which is defined as the ratio between the ultimate moment of the strengthened beams and that of the unstrengthened control beam at the central support. The bending moment was calculated based on satisfying the equilibrium conditions using the measured central support reaction and the applied load at the mid-spans. By comparing the ultimate load enhancement ratio, γ, (Table 8) of a strengthened beam and the ultimate moment enhancement ratio, μ, (Table 11) of a strengthened section in the same beam, it can be concluded that the latter was significantly higher than the former. Such a conclusion is not valid for simply supported beams strengthened with external reinforcement where the ultimate moment and load enhancement ratios are similar. All strengthened beams resisted higher moments than the control beam. For the tested beams E30NA, E50NA, E30NB and E5NB, the moment enhancement ratio of 1.80, 2.06, 1.91 and 2.09 is obtained respectively in comparison with the CB.

Figs. 15 and 16 show the total applied load plotted against the sagging and hogging bending moments for the tested beams. The hogging and sagging bending moments obtained from an elastic analysis based on assuming uniform flexural stiffness along the beam span are also plotted in Figs. 15 and 16. The behavior of all beams at early load levels was nearly elastic. For the control beam, by increasing the applied load, many cracks occurred, the steel reinforcement yielded, and consequently, the bending moment was found different from that calculated based on an elastic analysis, as can be seen from Figs. 15 and 16. The hogging bending moments of CB was always less than the elastic prediction, and the reverse was true for the strengthened beams.

3.5 Evaluation of moment redistribution

For the tested beams, the moment redistribution ratio β is calculated based on Eq. (5) and is given in Table 11. It was calculated for the positive and the negative moment at the mid-span and at the central support region (Figs. 15 and 16) at the failure load.

$$\beta = \frac{M_{el} - M_{ex}}{M_{el}} \times 100 \tag{5}$$

Where, M_{el} and M_{ex} are the elastic and the failure experimental moments respectively. The M_{el} in beams (with and without the strengthening laminates) was obtained from linear elastic analysis by assuming a constant flexural stiffness along the beams.

It is worth mentioning that the values of ultimate moment at the central support and at the mid-span region were determined for each incremental loading stage on the basis of the values of the applied load and the support reactions measured by the load cells.

Table 11 Redistribution of moment at failure

Beam no.	M_u (kN.m)	μ	β, (%)	
			Hogging region	Sagging region
CB	-36.11	1	38.15	-22.89
E30NA	-65.06	1.80	-4.68	3.33
E50NA	-74.38	2.06	-10.62	6.37
E30NB	-68.79	1.91	-3.98	2.34
E50NB	-75.35	2.09	-7.52	4.51

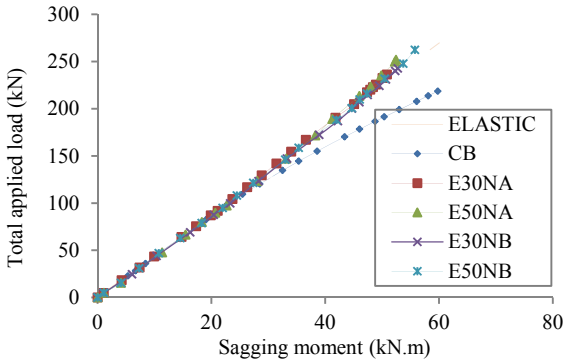

Fig. 15 Load versus positive moment at the mid-span region

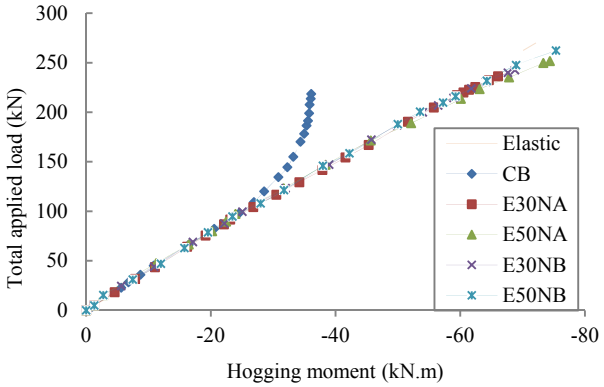

Fig. 16 Load versus negative moment at the central support region

The sagging bending moment of the strengthened beam was always smaller than the elastic predictions and the reverse was true for CB beam at the mid-span region (Figs. 15 and 16). Hence, the highest moment redistribution value was observed in CB with a moment redistribution ratio of 38.15% at the central support and 22.89% at the mid-span.

Considering Figs. 15 and 16 and Table 11, the moment redistribution ratio was found to depend on the existence of the CFRP laminate and its area. In the strengthened beams, the first crack occurred at the mid span region and unlike the CB, the moment was then transferred to the central support region. This may be attributed to the variation of the flexural stiffness along the beam. In other words, the CFRP laminate in the hogging region tends to attract moments to the central support due to a considerable enhancement in flexural stiffness. The moment redistribution ratio of the strengthened beams significantly decreased due to the increase in area of CFRP laminate. For beams, E30NA, E50NA, E30NB, and E50NB, moment redistribution ratios of -5.38%, -10.62%, -3.98% and -7.52% at the central support and 3.33%, 6.37%, 2.34% and 4.51% at mid span, were obtained respectively. By comparing the results for group B and group A, it was observed that the use of B anchorage system slightly increased the moment redistribution ratio as group B experienced higher rotation at the central support before failure than group A due to lack of slippage in the laminate.

4. Conclusions

In this study, experiments were performed on four continuous unbonded post-tensioned HSC beams retrofitted by end-anchored CFRP laminate in addition to a control beam, CB. The major results obtained include:

• In unbonded post-tensioned beams, an externally bonded reinforcement strengthening system can significantly improve the flexural performance at the serviceability state; while, based on result of previous researches, bonded prestressed concrete beam is not like that.

• The load at which the internal steel reinforcement for a strengthened beam yielded was between 16% and 48% higher than that of the corresponding steel reinforcement in the un-strengthened control beam yielded. This again highlights the existence of a much improved serviceability response.

• The cracking load for the strengthened beams increased by up to 56% comparing to the control beam. This allowed a reduction of crack amplitudes and a more uniform distribution of cracks. Besides, in the strengthened beams, the strain within the concrete compressive region was reduced as a result of smaller beam rotation at the central support. Reducing the size of cracks and the more uniform distribution are both desirable in bridge rehabilitation scenarios where deleterious agents can affect bridge durability in the long run.

• Reduction of the mid span deflection at the ultimate load due to the application of FRP was sizable for the strengthened beams. Similarly a large increase was observed in the value of the load corresponding to the allowable deflection which experienced an increase up to %58.

• Proper installation of CFRP and allowing adequate size for end anchorage are two important issues affecting the performance of the strengthening system. Allowing for adequately large dimensions of end anchorage, would help delaying end anchorage failures and increase the ultimate strain developable in the laminates even after their complete debonding. The ultimate CFRP strain in group B anchorages was significantly higher than that in group A. The overall average CFRP strains at ultimate for the strengthened beams using two different areas of CFRP laminate and end anchorage were 9600 $\mu\varepsilon$-6833 $\mu\varepsilon$.

• In the CB, after an initial phase of linear behavior to cracking, the deviation from elastic behavior was observed. On the contrary, the flexural behavior of the strengthened beams remained linear to failure.

• Failure of the beams occurred by concrete crushing at the central support and mid span and also end-anchorage failure after FRP debonding. This was the common method of failure observed in all beams.

• Depending on the area of CFRP laminate and end anchorage type, the increase in load capacity varied between a minimum of 8% and a maximum of 20% and the moment enhancement ratio at the central support varied between a minimum of 80% and a maximum of 109% for the strengthened beams. Meanwhile, increasing the CFRP area significantly decreased the moment redistribution ratio from 38.15% to-10.62% in the unstrengthened and strengthened beams respectively. This reconfirms the fact the system remains in the linear service state longer.

Overall, the main point to raise based on the findings is that the enhancements realized due to the suggested strengthening scheme affect the serviceability response considerably more than it affects the ultimate. This is the immediate outcome of the tendons being unbonded. The method is useful for bridges suffering from service overloads and cracking. The study is a new contribution to this research filed because i) the study is on two-span continuous beams which had not been studied previously by others and ii) it proves that the suggested strengthening will be considerably more effective for serviceability state rather than ultimate.

Acknowledgements

The authors would like to acknowledge Khansar metal industries for providing the PC strand and also Mr. Amin R Dortajnejad and Hamze Karamoziyan for assisting in the construction of the specimens. Acknowledgement is also due to the Faculty of Civil Engineering at the Shahid Bahonar University of Kerman for providing the laboratory test facilities.

References

ACI Committee 318 R (2011), *Building Code Requirements for Structural Concrete and Commentary*, American Concrete Institute, Farmington Hills, MI.

ACI Committee 440.2R (2008), *Guide for the Design and Construction of Externally Bonded FRP Systems for Strengthening Concrete Structures*, American Concrete Institute, Detroit, MI, 76p.

Akbarzadeh Bengar, H. and Maghsoudi, A.A. (2010), "Experimental investigations and verification of debonding strain of RHSC continuous beams strengthened in flexure with externally bonded FRPs", *Mater. Struct*., **43**, 815-837.

Akbarzadeh, H. and Maghsoudi, A.A. (2010), "Experimental and analytical investigation of reinforced high strength concrete continuous Beams strengthened with fibre reinforced polymer", *Mater. Des*., **31**, 1130-1147.

ASTM 370A (2012), *Standard Test Methods and Definitions for Mechanical Testing of Steel Products*, American society for testing and materials (ASTM), West Conshohocken, USA.

Bank, L.C. and Arora, D. (2006), "Analysis of RC beams strengthened with mechanically fastened FRP (MF-FRP) strips", *Compos. Struct.,* **79**, 180-191.

Breña, S.F., Bramblett, R.M., Wood, S. and Kreger, M. (2003), "Increasing flexural capacity of reinforced concrete beams using carbon fiber-reinforced polymer composites", *ACI Struct. J.*, **100**(1), 36-46.

BS 8110 (1997), *Structural Use of Concrete*, Part 1, British Standards Institution, Milton Keynes, UK.

BS EN 12390-3 (2009), *Testing hardened concrete. Compressive strength of test specimens,* British standards institution, Milton Keynes, UK.

Chahrour, A. and Soudki, K. (2005), "Flexural response of reinforced concrete beams strengthened with end-anchored partially bonded carbon fiber-reinforced polymer strips", *J. Compos. Constr.*, ASCE, **9**(2), 170-177.

Chakrabari, P.R. (2005), "Behavior of un-bonded post-tensioned beams repaired and retrofitted with composite materials", *ASCE Structures Congress*, Metropolis and Beyond, NY, April.

El-Meski, F. and Harajli, M. (2012), "Flexural behavior of unbonded post-tensioned concrete members strengthened using external frp composites", *J. Compos. Constr*., ASCE, **17**(2), 197-207.

El-Refaie, S.A., Ashour, A.F. and Garrity, S.W. (2003), "Sagging and hogging strengthening of continuous reinforced concrete beams using carbon fiber-reinforced polymer sheets", *ACI Struct. J*., **100**(4), 446-453.

Farahbod, F. and Mostofinejad, D. (2010), "Experimental study of moment redistribution in RC frames strengthened with CFRP sheets", *Compos. Struct*., **93**, 1168-1177.

Foret, G. and Limam, O. (2008), "Experimental and numerical analysis of RC two-way slabs strengthened with NSM CFRP rods", *Constr. Build. Mater.*, **22**, 2025-2030.

Garden, H.N. and Hollaway, L.C. (1998), "An experimental study of the influence of plate endanchorage of carbon fibre composite plates used to strengthen reinforced concrete beams", *Compos. Struct*., **42**, 175-188.

Ghasemi S. (2012), "Behavior of continuous un-bounded post-tensioned concrete members strengthened with cfrp laminates (Experimental Investigation)", MSc Dissertation, Shahid Bahonar University of Kerman, Kerman, Iran.

Iranian concrete code (Mabhas 9) (2009), *Design and Construction of Reinforced Concrete Buildings*, National Building Codes, Tehran, Iran.

Klaiber F.W. and Wipf T.J. (2003), "Repair of damaged prestressed concrete bridges using CFRP", *Proceeding of M.C.T.R. Symposium*, Ames, Iowa State University.

Lamanna, A.J., Bank, L.C. and Scott, D.W. (2001), "Flexural strengthening of reinforced concrete beams using fasteners and fiber-reinforced polymer strips", *ACI Struct. J.*, **98**(3), 368-376.

Lignola, G.P., Prota, A., Manfredi, G. and Cosenza, E. (2007), "Experimental performance of RC hollow columns confined with CFRP", *J. Compos. Constr*., ASCE, **11**(1), 42-49.

Meier, U., Deuring, M., Meier, H. and Schwegler, G. (1993), *Strengthening of Structures with Advanced Composites, Alternative Materials for Reinforcement and Prestressing of Concrete*, Clarke/Chapman & Hall, Glasgow, Scotland.

Mirmiran, A., Shahawy, M., Nanni, A. and Karbhari, V. (2004), "Bonded repair and retrofit of concrete structures using FRP composites", National Cooperative Highway Research Program (NCHRP) Report 514, Transportation Research Board.

Pellegrino, C. and Modena, C. (2009), "Flexural strengthening of real-scale rc beams with end-anchored pretensioned frp laminates", *ACI Struct. J.*, **106**(3), 319-328.

Rosenboom, O., Hassan, T.K. and Rizkalla, S. (2007), "Flexural behavior of aged prestressed concrete girders strengthened with various FRP systems", *Constr. Build. Mater*., **21**, 764-776.

Rosenboom, O., Walter, C. and Rizkalla, S. (2009), "Strengthening of prestressed concrete girders with composites: Installation, design and inspection", *Constr. Build. Mater*., **23**, 1495-1507.

Schiebel, S., Parretti, R. and Nanni, A. (2001), "Repair and strengthening of impacted PC girders on bridge A4845", Missouri Department of Transportation Report RDT01-017/RI01-016.

Takács, P.F. and Kanstad, T. (2002), "Strengthening prestressed concrete beams with carbon fiber reinforced polymer plates", NTNU Report R-9-00, Norway.

Teng, J.G., Chen, J.F., Smith, S.T. and Lam, L. (2002), *FRP Strengthened RC Structures*, Wiley, New York.

Warwaruk, J., Sozen, M.A. and Siess, C.P. (1962), "Investigation of prestressed concrete for highway bridges, part III: strength and behavior in flexure of prestressed beams", Bulletin No. 464, Engineering Experiment Station, University of Illinois, Urbana.

CC